

The Electronic Properties of a Model Active Site for Blue Copper Proteins as Probed by Stark Spectroscopy

Arindam Chowdhury and Linda A. Peteanu*

Department of Chemistry, Carnegie Mellon University, Pittsburgh, Pennsylvania 15213

Patrick L. Holland and William B. Tolman

Department of Chemistry, University of Minnesota, 207 Pleasant Street SE, Minneapolis, Minnesota 55455

Received: April 26, 2001; In Final Form: November 7, 2001

A complex that mimics many of the properties of the blue copper protein center that was synthesized by Holland and Tolman¹ is studied using Stark spectroscopy to determine the values of two electronic properties, the change in the dipole moments ($|\Delta\mu|$) and the average change in the polarizability ($\langle\Delta\alpha\rangle$) for excitation into the ligand-to-metal charge transfer (LMCT) band. Measurements at 77 K in methylcyclohexane yield a value for $|\Delta\mu|$ of between 1.3 and 1.9 D for the lowest energy LMCT band, which has been assigned as a predominantly thiolate ($S\pi$) \rightarrow Cu($d_{x^2-y^2}$) transition.² The value of $|\Delta\mu|$ is remarkably similar to that we have measured earlier for the type-1 blue copper protein azurin in a glycerol–water glass. The sensitivity of Stark spectroscopy to charge-transfer transitions is utilized to identify and, in some cases, to confirm the assignment previously made via magnetic circular dichroism (MCD)² of several higher-energy charge-transfer bands. Values for the electron-transfer matrix element (H_{ab}) and the effective charge-transfer distance (R_{ab}) derived from our measurements on this complex are also reported. These parameters are likewise found to be quite similar to those previously determined for azurin.

Introduction

The type-1 class of blue copper proteins (bcp's) are involved in biological electron transfer in photosynthesis and in respiration.³ Their active sites share the structural motif of three strongly coordinating ligands, two histidines and a cysteine, bound to the central copper that is in its 2^+ oxidation state. However, among bcp species, numerous variants of the coordination geometries of the active site are seen. These include trigonal bipyramidal in azurin, which contains two weakly coordinating residues, distorted tetrahedral for plastocyanin, which contains a single residue at shorter distance (2.1 Å), and trigonal planar for proteins such as ceruloplasmin, fungal laccase, and some azurin mutants, in which axial ligation is absent. Nonetheless, all are characterized by a short (~ 2.1 Å) Cu–S bond that is the primary source of many of their characteristic spectroscopic features, including their color, which is due to an intense charge-transfer band in the ~ 620 nm region.³ Regarding function, this Cu–S bond is proposed to serve as a favorable conduit for biological electron transfer.⁴

One of the prime topics of interest in the study of bcp's is the manner in which the coordination of the Cu site affects the spectroscopy and, by inference, the electron-transfer properties of these systems. This interplay has been explored in great detail via comparisons between bcp's with different active site geometries as well as by using site-directed mutagenesis and the addition of exogenous ligands to modify the active site.^{5–10} Moreover, comparison of the spectroscopic and redox properties of bcp's to those of typically square planar *synthetic* Cu²⁺ species led to the proposal that the unique geometry of the protein Cu site is optimized both to reduce the reorganization energy associated with electron transfer and to increase the

covalency of the Cu–S bond, meaning that the valence electron is nearly equally distributed over the Cu and S sites. The latter effect is thought to enhance the coupling of the Cu center to the protein backbone via the S and to thereby provide a favorable pathway for ground-state electron transfer.³

For many years, inorganic copper complexes with properties similar to those of the type-1 Cu proteins were unknown in the literature. However, recently, several complexes have been synthesized that mimic the distorted tetrahedral¹¹ and trigonal planar¹ coordination geometries found in the Cu proteins. Spectroscopic studies of these complexes allow the relationship between the identity of the coordinating ligands and the properties of the Cu site to be examined.^{2,6,12} On the basis of electron spin resonance (ESR), magnetic circular dichroism (MCD), and resonance Raman measurements of these synthetic complexes, Solomon and co-workers have delineated several similarities as well as differences between the protein and synthetic systems.^{2,12}

In this communication, we report an electroabsorption (Stark) spectroscopic study of the complex shown in Figure 1a (referred to here as **1**) that was recently synthesized by Holland and Tolman.¹ This system is a structural model of the active sites of trigonal planar type-1 copper proteins, such as fungal laccase. Electroabsorption (Stark) spectroscopy is frequently applied to the study of intramolecular electron transfer in organic, inorganic, and biological systems^{13–18} because it provides a quantitative measure of the extent of charge transfer in the excited state as compared to the ground state of a molecule via $|\Delta\mu|$, the absolute value of the change in dipole moment. This quantity, in turn, can be used to evaluate the electronic matrix element for electron transfer in the system (H_{ab}) as described in ref 19. In addition, the average change in the polarizability ($\langle\Delta\alpha\rangle$) between the lower and upper states of the optical

* To whom correspondence should be addressed. E-mail: peteanu@andrew.cmu.edu.

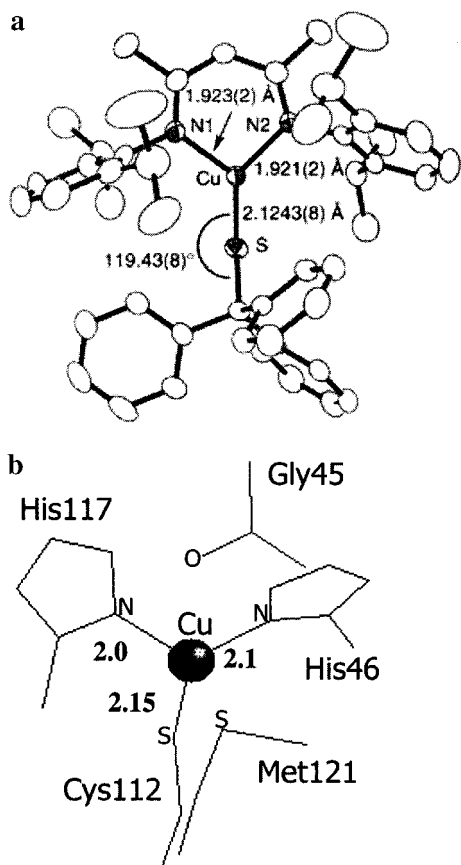


Figure 1. The structure of complex **1** (a) and the active site of azurin (b). The ligands surrounding the copper center and the bond distances (Å) between the copper and the ligands coplanar to it are shown. The structures are reproduced from ref 1 and 28, respectively.

transition is measured. The trace of the polarizability of a state i is proportional to $\sum_{j \neq i} |\bar{\mu}_{ij}|^2 / (E_j - E_i)$, where $\bar{\mu}_{ij}$ represents the transition moment between electronic state i and all other states j and E represents the energy of the respective states. Therefore, the quantity $\langle \Delta\alpha \rangle$ reflects the interactions between the electronic states that are coupled in the optical transition and *all* other electronic states of the system. It is also frequently regarded as a measure of the change in the extent of electron delocalization upon optical excitation. For example, a large positive value of $\langle \Delta\alpha \rangle$ is often interpreted to imply greater electron delocalization in the excited state than in the ground state of the optical transition.

The information contained in both $|\bar{\Delta\mu}|$ and $\langle \Delta\alpha \rangle$ complements other spectroscopic and electronic structure studies of **1** in the literature.² Here, we report these quantities for several charge-transfer transitions identified in the absorption spectrum of **1** and compare these results to those obtained previously for two species of azurin.¹⁷ This comparison indicates a high degree of similarity between the electronic properties of the main charge-transfer band of **1** and the corresponding transition of the azurins, indicating that the synthetic complex successfully mimics this aspect of the electronic structure of the bcp's as well.

Experimental Section

Compound **1** was synthesized by Holland and Tolman as reported in ref 1. This complex is oxygen sensitive and was therefore handled in the nitrogen atmosphere of a glovebox. The solvent, 2-methylcyclohexane (MCH, Aldrich), was dried over CaH_2 in an argon atmosphere and degassed by freeze-

thaw methods to remove oxygen prior to dissolving **1**. Samples for electroabsorption were prepared in the glovebox by placing a drop of this solution between two indium tin oxide (ITO)-coated glass slides, which are then clipped together with a 50 μm thick Kapton film used as a spacer between the two electrodes. Immediately after removal from the oxygen-free atmosphere, the cell was inserted in a liquid nitrogen optical Dewar flask (H. S. Martin) to form a glass, ensuring that the complex was not exposed to air for more than 1 min. An AC electric field of 2500 V (~ 470 Hz) was applied to the glass, and electroabsorption measurements were performed using a home-built Stark spectrometer, which is described fully in ref 20. The transmission spectrum of the complex was measured at the same time as the electroabsorption spectrum and converted to an absorption spectrum using a blank consisting of MCH glass between ITO electrodes. Room-temperature absorption spectra of the same solution of **1** used for the electroabsorption measurements were also recorded using a Perkin-Elmer absorption spectrophotometer from 400 to 1000 nm to compare to published data.

Data Analysis Procedures. The analysis of the electroabsorption data follows that in the literature.²¹ The equations shown here are appropriate for the experimental conditions used, that is, the sample is isotropically oriented within a rigid glass. Essentially, the change in absorption due to the application of an external electric field is fit to the weighted sum of zeroth, first, and second derivatives of the zero-field absorption spectrum. The overall change in absorbance caused by the application of an electric field can be described by the following equation:

$$\Delta A(\tilde{\nu}) = \bar{F}_{\text{eff}}^2 \left[\mathbf{a}_\chi A(\tilde{\nu}) + \mathbf{b}_\chi \frac{\tilde{\nu}}{15\hbar} \left\{ \frac{\partial}{\partial \tilde{\nu}} \left(\frac{A(\tilde{\nu})}{\tilde{\nu}} \right) \right\} + \mathbf{c}_\chi \frac{\tilde{\nu}}{30\hbar^2} \left\{ \frac{\partial^2}{\partial \tilde{\nu}^2} \left(\frac{A(\tilde{\nu})}{\tilde{\nu}} \right) \right\} \right] \quad (1)$$

The $A(\tilde{\nu})$ represents the unperturbed absorption as a function of frequency ($\tilde{\nu}$) and \bar{F}_{eff} represents the field at the sample in V/cm. This effective field includes the enhancement of the applied field due to the cavity field of the matrix. The subscript χ represents the angle between the direction of the applied electric field and the electric field vector of the polarized light. The experiment is normally performed at two angles, $\chi = 54.7^\circ$ (magic angle) and $\chi = 90^\circ$. In the laboratory frame, this angle is actually set to 46° to account for the refractive index of liquid nitrogen and of the solvent glass. Because the refractive index of the glass is not precisely known, we use the ratios of the sample absorbances at the two angles to verify that the laboratory frame angle has been set correctly to yield a value of χ of 54.7° at the sample.^{14,17}

The expressions of \mathbf{a}_χ , \mathbf{b}_χ , and \mathbf{c}_χ are related to the change in the transition moment polarizability (A_{ij}) and hyperpolarizability (B_{ij}), the change in the electronic polarizability ($\langle \Delta\alpha \rangle$), and the change in the dipole moments ($|\Delta\mu|$), respectively, as given in eqs 2–4 below.

$$\mathbf{a}_{54.7} = \frac{1}{3|\bar{m}|^2} \sum_{ij} A_{ij}^2 + \frac{2}{3|\bar{m}|^2} \sum_{ij} m_i B_{ij} \quad (2)$$

$$\mathbf{b}_{54.7} = \frac{10}{|\bar{m}|^2} \sum_{ij} m_i A_{ij} \Delta\mu_j + \frac{15}{2} \langle \Delta\alpha \rangle \quad (3)$$

$$\mathbf{c}_{54.7} = 5|\bar{\Delta\mu}|^2 \quad (4)$$

In the above equations, the tensors $\underline{\mathbf{A}}$ and $\underline{\mathbf{B}}$ represent the transition polarizability and hyperpolarizability, respectively. These terms are generally small for allowed transitions and can therefore be neglected relative to other terms in the expression for $\langle \Delta\alpha \rangle$ (eq 3), particularly in those compounds exhibiting a small value of $|\Delta\mu|$, such as that reported here for **1** and previously for other bcp's.¹⁷

Information regarding $|\Delta\mu|$ for the molecule is contained in the $c_{54.7}$ term (eq 4). It is important to emphasize that, for an isotropic sample such as those studied in this work, only the magnitude and not the sign of $\Delta\mu$ is measured.

Performing the experiment at any different angle, χ , in our case 90° , allows us to estimate the relative orientation of the $|\Delta\mu|$ with respect to the transition dipole moment direction. If the ratio of coefficient c_χ at 54.7° versus 90° is ~ 1.67 , one can infer that the transition moment vector ($\vec{\mu}$) is parallel to the direction of $\Delta\mu$ for the transition. For further discussion, see ref 17.

The coefficients, \mathbf{a}_χ , \mathbf{b}_χ , and \mathbf{c}_χ , are extracted by means of a linear least-squares (LLSQ) fit of the electroabsorption signal to the sum of the derivatives of $A(\tilde{\nu})$. If the resultant fit to the absorption line shape (a single set of \mathbf{a}_χ , \mathbf{b}_χ , and \mathbf{c}_χ) is not of high quality, this is an indication that there is more than one transition (electronic or vibronic) underlying the absorption band, each having different electrooptical properties ($|\Delta\mu|$ and/or $\langle \Delta\alpha \rangle$). This is the case for the electroabsorption spectra of both bcp's studied previously¹⁷ and for **1** as presented here.

In such instances, one strategy to the fit to the electroabsorption spectrum is to model the underlying transitions in the absorption band as a sum of Gaussians. To implement this method, we chose the starting parameters for the bands to fit the absorption spectrum of **1** to be those Gaussians used to fit the 4 K magnetic circular dichroism (MCD) data by Solomon et al.² The initial parameters were varied using a simplex routine to obtain the best fit to the absorption spectrum using a minimum number of Gaussians. The final parameters for all Gaussians used to model the absorption of **1** at 77 K are summarized in Table 1 of the Supporting Information. Values of \mathbf{a}_χ , \mathbf{b}_χ , and \mathbf{c}_χ for each individual Gaussian or sums of different sets of Gaussians were then evaluated through the fitting procedure. By using these coefficients and eqs 3 and 4 above, a value of $|\Delta\mu|$ and $\langle \Delta\alpha \rangle$ was assigned to each transition. This method is explained in detail in ref 22.

A second strategy, also used here, is to subdivide the absorption and electroabsorption spectra into regions, which are then each fit using a single set of \mathbf{a}_χ , \mathbf{b}_χ , and \mathbf{c}_χ parameters.²³ Selecting the regions to be fit is normally a matter of trial and error though an effort is made to maximize the wavenumber range of each region chosen. One advantage of this method of fitting to the truncated absorption spectrum over the Gaussian resolution approach described above is that the number of fitting parameters is significantly reduced. Possible artifacts arising from the fitting of overlapping Gaussian bands are also minimized.

To summarize, the two quantities derived from the Stark spectrum reported here are the values of $|\Delta\mu|$ and $\langle \Delta\alpha \rangle$ for each of the bands in the absorption spectrum of **1** that exhibit a significant field response. Note that the experimentally reported values have not been corrected for the effects of the cavity and reaction field. For a more detailed discussion of the analysis method, see refs 15 and 21.

Results and Discussion

Results of Fitting the Electroabsorption Spectrum. The absorption spectra of **1** in MCH at 300 and 77 K are shown in

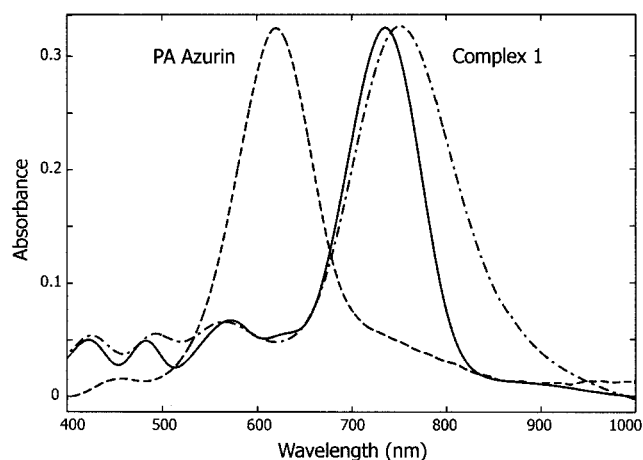


Figure 2. Room temperature (dashed-dot line) and 77 K (solid line) absorption spectra of **1** in methylocyclohexane. For comparison, the absorption spectrum of the type-I blue copper protein PA azurin (dashed lines) in 50% glycerol–water glass at 77 K is shown.

Figure 2. The spectra are characterized by an intense transition at ~ 740 nm and several weaker transitions between 400 and 650 nm. Upon lowering the temperature, the maximum of the most intense transition shifts 270 cm^{-1} to higher energy and the band becomes more highly resolved. Two transitions located at higher energy (~ 490 and ~ 430 nm) exhibit a similar blue shift ($\sim 200\text{ cm}^{-1}$) at 77 K relative to 298 K, while the position of the band at ~ 570 nm is essentially unchanged.

Using MCD spectroscopy, Solomon and co-workers have shown that the most intense transition of **1** at ~ 750 nm arises from charge transfer *predominantly* from the thiolate (S) π orbital to the $\text{Cu}(d_{x^2-y^2})$ orbital and will be referred to in this fashion throughout though the N atoms of the ligand *also* act as donors.² Likewise, the strongest band (~ 620 nm) in azurin and other bcp's arises from the $\text{Cys}(S\pi) \rightarrow \text{Cu}(d_{x^2-y^2})$ ligand-to-metal charge-transfer (LMCT) transition.² The assignments of the remaining bands will be considered in more detail below.

The electroabsorption signal of **1** is shown in Figure 3b (solid line). The signal intensity for the thiolate ($S\pi$) \rightarrow $\text{Cu}(d_{x^2-y^2})$ LMCT transition is comparable to that observed for azurin.¹⁷ However, the electroabsorption signal is *much stronger* for **1** in the high-energy region ($19\,000$ – $24\,000\text{ cm}^{-1}$) where the absorption itself is relatively *weak*. This demonstrates that the various underlying transitions have different values of $|\Delta\mu|$ or $\langle \Delta\alpha \rangle$ or both.

In this work, we take two approaches to fitting the electroabsorption spectrum of **1** (see Experimental Section). One is to model the absorption spectrum with several Gaussian bands and to allow the fitting parameters of each ($\mathbf{a}_{54.7}$, $\mathbf{b}_{54.7}$, and $\mathbf{c}_{54.7}$ of eqs 2–4) to vary independently. A minimum of seven Gaussian bands (G1–G7 in Figure 3a) was required to fit the absorption spectrum in the region shown. Their assignments will be discussed following a description of the fitting results.

In the low-energy region, a high-quality fit to the electroabsorption spectrum (Figure 3b) was obtained by this method. The fit shown in Figure 3b yields 1.9 ± 0.3 D for $|\Delta\mu|$ and $-15 \pm 5\text{ \AA}^3$ for $\langle \Delta\alpha \rangle$ for G2 and similar values for G3 (Table 1). The magnitudes of $|\Delta\mu|$ measured for G2 and G3 indicate that *both* have some charge-transfer character.

The second approach is to truncate the electroabsorption spectrum into distinct wavelength regions that are then fit independently using the corresponding regions of the experimental absorption spectrum. While this method (truncated fit, Figure 3c) gives a somewhat lower-quality fit to the data, the

TABLE 1: Electroabsorption Results for the LMCT Transitions of 1

	truncated absorption ^a	Gaussians ^b		truncated absorption ^a	Gaussians ^b		truncated absorption ^a	Gaussians ^b	
		G2	G3		G4	G5		G6	G7
frequency ^c	11 500–15500	13 550	14 640	16 000–19 000	15 830	17 560	19 500–25 000	20 700	23 620
$ \Delta\mu $ ^d	1.3 (0.2)	1.9 (0.3)	1.2 (0.3)	2.0 (0.2)		3.6 (0.4)		2.6 (0.5)	7.6 (1.0)
$\langle\Delta\alpha\rangle$ ^e	1 (2)	−15 (5)	−10 (4)	10 (2)		24 (10)		45 (5)	55 (12)

^a Fit using the truncated absorption. ^b Fit using independent Gaussians. ^c Reported in cm^{-1} . ^d Reported in D. ^e Reported in \AA^3 . Errors are in parentheses.

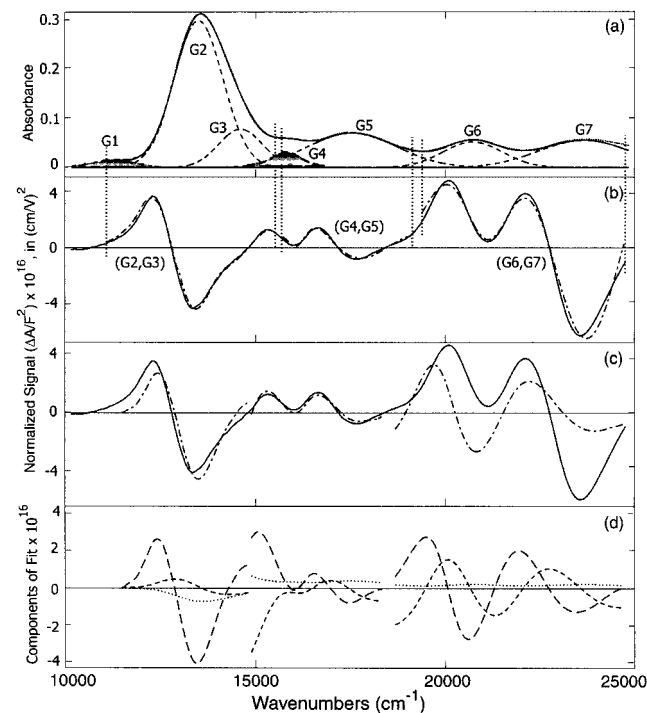


Figure 3. Absorption and electroabsorption spectra for **1**. The absorption spectrum of **1** (panel a) was modeled using seven Gaussians (dashed line) marked G1–G7. G1 and G4 are shaded for clarity. The experimental absorption spectrum (dotted) lies below the sum of the gaussians (solid). The vertical dashed lines indicate the various ranges of the electroabsorption signal that were fit as indicated in Table 1. The parameters for the Gaussians are contained in the Supporting Information. Panel b contains the experimental electroabsorption spectrum (solid lines) normalized by the square of the applied electric field at the magic angle, $\chi = 54.7^\circ$. The fits to the electroabsorption signal (dashed-dot lines) shown here were obtained using the Gaussians shown in panel a. The bands in parentheses denote the particular Gaussians that were used to fit each of the three regions shown. Panel c contains the fit obtained by dividing the electroabsorption spectrum into three regions and fitting each separately to the corresponding region of the experimental absorption spectrum (truncated fit, see text). Panel d contains the decomposition of the fit shown in panel c into the zeroth (dotted), first (short dash), and second derivative (long dash) contributions. The decomposition of the fit in panel b is contained in the Supporting Information.

value obtained for $|\overline{\Delta\mu}|$ is similar to that obtained via the fit to Gaussians (Table 1) though the value of $\langle\Delta\alpha\rangle$ is not. The discrepancy in $\langle\Delta\alpha\rangle$ probably arises because the values of $\langle\Delta\alpha\rangle$ obtained using the Gaussian fitting method in this region proved to be quite sensitive to the parameters used though the values of $|\overline{\Delta\mu}|$ were not.

In the intermediate region of the electroabsorption spectrum, a good fit could be obtained using both the truncated absorption spectrum and the Gaussian resolution method (Table 1). The electronic properties of G4 were not reported, however, because this band has a very small oscillator strength.

Finally, the electroabsorption spectrum in the high-energy region (19 000–25 000 cm^{-1}) can *only* be obtained by varying

the parameters of Gaussians G6 and G7 independently. The truncated fit completely fails to reproduce the line shape of the electroabsorption signal (Figure 3c). Consistent with the strong field response seen in this wavelength region, band G7 exhibits a *substantially larger* value of $|\Delta\mu|$ (7.6 D) than does the low-energy LMCT band (G2). Our results support the previous assignment of G7 as an LMCT band.² However, they *also* indicate that G6 has charge-transfer character, suggesting that this transition may *not* be of d–d origin as it had been assigned in ref 2.

It is possible to evaluate the angle between the transition dipole moment and $\Delta\mu$ by obtaining the electroabsorption at two different angles of χ (i.e., 54.7° and 90° , see ref 17). We obtain values for $c_{54.7}/c_{90}$ of $\sim 1.67 (\pm 0.2)$ for both the thiolate ($S\pi \rightarrow \text{Cu}(d_{x^2-y^2})$) LMCT transition (equivalent to G2) and the higher-energy transitions (G6 and G7). Therefore, $\Delta\mu$ is nearly parallel to the direction of the transition dipole moment in all three transitions. This result for the thiolate ($S\pi \rightarrow \text{Cu}(d_{x^2-y^2})$) LMCT band of **1** is very similar to that obtained from electroabsorption spectroscopy of the analogous transition in azurin.¹⁷

Assignments of the Bands Comprising the Absorption Spectrum of 1. To turn to assignments of the transitions described above, these will be discussed within the framework of the published assignments of Solomon and co-workers (specifically, Figure 2A and Table 1 of ref 2). As stated earlier, Gaussian G2 in the spectrum of **1** corresponds to the most intense thiolate $S(p,\pi) \rightarrow \text{Cu}(d_{x^2-y^2})$ LMCT transition.² Gaussian G7 is nearest in energy to a band assigned previously to a second LMCT transition.² This is also consistent with its large value of $|\Delta\mu|$ (Table 1). Two possible origins for this LMCT transition were considered in ref 2, one from the thiolate $S(p,\text{pseudo-}\sigma) \rightarrow \text{Cu}$ and the second arising from the nitrogen ($\text{N} \rightarrow \text{Cu}$) of the β -diketiminato ligand (Figure 1a). However, the former was argued to be more consistent with a variety of other spectroscopic measurements.² Bands in the region of G4–G6 have been assigned as Cu d–d transitions via MCD.² However, we measure significant values of $|\Delta\mu|$ for these, indicating charge-transfer character. In addition, as described above, our results point to there being a second charge-transfer transition in the high-energy region of the spectrum corresponding to G6 that is *not* evident from the MCD spectrum of ref 2. Finally, band G3, which *also* has considerable charge-transfer character, has no obvious analogue in the Gaussian resolution of the absorption spectrum used to fit the MCD data.² In summary, the results of Stark spectroscopy are in generally good agreement with MCD data² regarding the positions of the LMCT bands of **1**, though several additional transitions with significant charge-transfer are identified uniquely in the Stark spectrum.

Comparison of the Properties of 1 to Those of Azurin. The most intense band in azurin (~ 620 nm) is due to a $S(\pi) \rightarrow \text{Cu}(d_{x^2-y^2})$ LMCT arising from the cysteine ligand.^{24,25} It shows a $|\Delta\mu|$ of 1.8 ± 0.5 D and a $\langle\Delta\alpha\rangle$ of -15 ± 5 \AA^3 .¹⁷ The properties measured for the analogous transition (thiolate ($S\pi \rightarrow \text{Cu}(d_{x^2-y^2})$) of **1** (Table 1) are remarkably similar.

Randall et al. have proposed that the transition corresponding to G7 in **1** arises either from the S(p,pseudo- σ) \rightarrow Cu LMCT or from the N σ orbital of the β -diketiminato ligand with the former assignment being considered more likely.² Our results support their assignment for the following reason. In azurin, the field response of the Cys(S pseudo- σ) \rightarrow Cu($d_{x^2-y^2}$) LMCT transition is quite strong ($|\Delta\mu|$ and $\langle\Delta\alpha\rangle$ of 3–5 D and ~ 30 Å³, respectively),²⁶ whereas the high-energy His(N) \rightarrow Cu(II)-($d_{x^2-y^2}$) LMCT transitions^{24,25} have very weak responses to the applied field and therefore have much smaller values of $|\Delta\mu|$ and $\langle\Delta\alpha\rangle$.¹⁷ To the extent that it is reasonable to compare a LMCT transition arising from a histidine N in azurin with that arising from the N of a β -diketiminato ligand in **1**, the fact that the His(N) \rightarrow Cu(II)-($d_{x^2-y^2}$) LMCT is *weak* in the Stark spectrum of azurin supports the assignment² of the charge-transfer band of **1** in the region of G7 (~ 420 nm) to a S(p, pseudo- σ) \rightarrow Cu LMCT rather than to a nitrogen-based transition.

Electron-Transfer Parameters Derived from Stark Measurements. Using values obtained from electroabsorption measurements, one may obtain electron-transfer parameters such as the electron-transfer coupling element H_{ab} and the effective charge-transfer distance R_{ab} between the donor and the acceptor. For example, the quantity H_{ab} may be estimated from the transition dipole moment ($\vec{\mu}_{ij}$), the $|\Delta\mu|$, and the absorption maxima of the transition ($\bar{\nu}_{\max}$) using the following expression of Cave and Newton:¹⁹

$$H_{ab} = \frac{\vec{\mu}_{ij} \cdot \bar{\nu}_{\max}}{\sqrt{|\Delta\mu|^2 + 4|\vec{\mu}_{ij}|^2}} \quad (5)$$

We obtained the value of the transition dipole moment (2.6 D) of the most intense LMCT transition (12 000–15 000 cm⁻¹) of **1** by integrating the absorption spectrum at 77 K in this region ($\epsilon_{\max} = \sim 5700$ M⁻¹ cm⁻¹). Using the experimentally measured value of ~ 1.9 D for $|\Delta\mu|$ of this band and 13 550 cm⁻¹ for $\bar{\nu}_{\max}$, we obtained a value of H_{ab} of 6350 \pm 250 cm⁻¹. This value is indeed similar to the value that we had obtained previously for azurin (~ 7800 cm⁻¹).¹⁷ Such large values of H_{ab} reflect the fact that, for both systems, the electron is highly delocalized on the ground-state surface and electron transfer is essentially barrierless as a result.

It is also possible to estimate the effective charge-transfer distance R_{ab} for charge-transfer transitions from the change in the dipole moment as $R_{ab} = |\Delta\mu|/e$, where e is the charge of a single electron. For **1**, a value of ~ 10 D for $|\Delta\mu|$ would be measured if one full electron charge were to move across the crystallographic distance separating the Cu and S atoms (2.12 Å). Instead, we observe a much *smaller* value of $|\Delta\mu|$ suggesting that only partial charge transfer occurs on transition. If, in **1**, R_{ab} is considered to be the crystallographic distance between Cu and S atoms, our measured $|\Delta\mu|$ implies that ~ 0.19 e is transferred to the S upon photoexcitation. Alternatively, one can say that a full electron is transferred over a distance of 0.4 Å. These are very similar to the corresponding values obtained for azurin, for which it has been estimated that ~ 0.2 e is transferred on excitation.²⁷ Likewise, the measured $|\Delta\mu|$ of 1.7 D for azurin¹⁷ would imply that a full electron is transferred over 0.35 Å. These comparisons again emphasize the similarities between the thiolate (S, π) \rightarrow Cu($d_{x^2-y^2}$) LMCT transition of **1** and the analogous Cys(S π) \rightarrow Cu($d_{x^2-y^2}$) LMCT transition of the protein system.

Conclusions

Using Stark spectroscopy, we have demonstrated that the two electronic properties, $|\Delta\mu|$ and $\langle\Delta\alpha\rangle$, for the Cys(S, π) \rightarrow

Cu($d_{x^2-y^2}$) LMCT transitions of a synthetic compound designed to mimic several of the properties of the blue copper protein active site are remarkably similar to those previously reported by us for two species of azurin. While the value of $|\Delta\mu|$ for the lowest-energy (thiolate (S, π) \rightarrow Cu($d_{x^2-y^2}$)) LMCT transition of the complex is relatively small, values of up to ~ 8 D are observed for higher-energy charge-transfer transitions. The Stark spectrum shows general agreement with the published MCD spectrum of **1** regarding the positions of the various LMCT bands though *additional* charge-transfer transitions are identified in the Stark spectrum that have no obvious counterpart in the published Gaussian resolution of the absorption spectrum based on MCD data. This highlights the utility of employing multiple spectroscopic techniques to resolve and assign electronic absorption spectra containing overlapping transitions, such as that of the complex studied here. Finally, we derive a large value for electron-transfer matrix element, H_{ab} , from the measured properties of the thiolate (S, π) \rightarrow Cu($d_{x^2-y^2}$) LMCT band that is likewise similar in magnitude to the value that we previously reported for azurin.

Acknowledgment. L.A.P. and A.C. acknowledge our sources of funding, the NSF CAREER and POWRE programs, Dr. Colin Horwitz for permission to use his glovebox, and Dr. Sujit Mondal and Anindya Ghosh for help with sample handling. We also thank the Center for Molecular Analysis at Carnegie Mellon University for the use of the absorption spectrometer. W.B.T. and P.L.H. acknowledge NIH Grant GM47365.

Supporting Information Available: A table of Gaussian parameters and a graph of Gaussian resolutions. This material is available free of charge via the Internet at <http://pubs.acs.org>.

References and Notes

- Holland, P. L.; Tolman, W. B. *J. Am. Chem. Soc.* **1999**, *121*, 7270–7271.
- Randall, D. W.; DeBeer George, S.; Holland, P. L.; Hedman, B.; Hodgson, K. O.; Tolman, W. B.; Solomon, E. I. *J. Am. Chem. Soc.* **2000**, *122*, 11632–11648.
- Solomon, E.; Baldwin, M.; Lowery, M. *Chem. Rev.* **1992**, *92*, 521–542.
- Solomon, E. I.; Lowery, M. D. *Science* **1993**, *259*, 1575–1581.
- LaCroix, L. B.; Randall, D. W.; Nersissian, A. M.; Hoitink, C. W. G.; Canters, G. W.; Valentine, J. S.; Solomon, E. I. *J. Am. Chem. Soc.* **1998**, *120*, 9621–9631.
- Palmer, A. E.; Randall, D. W.; Xu, F.; Solomon, E. I. *J. Am. Chem. Soc.* **1999**, *121*, 7138–7149.
- Kroes, S. J.; Hoitink, C. W. G.; Andrew, C. R.; Ai, J.; Sanders-Loehr, J.; Messerschmidt, A.; Hagen, W. R.; Canters, G. W. *Eur. J. Biochem.* **1996**, *240*, 342–351.
- den Blaauwen, T.; Canters, G. W. *J. Am. Chem. Soc.* **1993**, *115*, 1121–1129.
- Pierloot, K.; De Kerpel, J. O. A.; Ryde, U.; Olsson, M. H. M.; Roos, B. O. *J. Am. Chem. Soc.* **1998**, *120*, 13156–13166.
- Di Bilio, A. J.; Chang, T. K.; Malmstrom, B. G.; Gray, H. B.; Karlsson, B. G.; Nordling, M.; Pascjer, T.; Lundberg, L. G. *Inorg. Chim. Acta* **1992**, *198–200*, 145.
- Kitajima, N.; Fujisawa, K.; Morooka, Y. *J. Am. Chem. Soc.* **1990**, *112*, 3210–3212.
- Randall, D. W.; DeBeer George, S.; Hedman, B.; Hodgson, K. O.; Fujisawa, K.; Solomon, E. I. *J. Am. Chem. Soc.* **2000**, *122*, 11620–11631.
- Oh, D. H.; Sano, M.; Boxer, S. G. *J. Am. Chem. Soc.* **1991**, *113*, 6880–6890.
- Shin, Y.-g.; Brunschwig, B. C.; Creutz, C.; Sutin, N. *J. Phys. Chem.* **1996**, *100*, 8157.
- Bublitz, G. U.; Boxer, S. G. *Annu. Rev. Phys. Chem.* **1997**, *48*, 213–242.
- Vance, F. W.; Karki, L.; Reigle, J. K.; Hupp, J. T.; Ratner, M. J. *Phys. Chem. A* **1998**, *102*, 8320–8324.
- Chowdhury, A.; Peteanu, L. A.; Webb, M. A.; Loppnow, G. R. *J. Phys. Chem. B* **2000**, *105*, 527–534.

- (18) Walters, K. A.; Premvardhan, L. L.; Liu, Y.; Peteanu, L. A.; Schanze, K. S. *Chem. Phys. Lett.*, in press.
- (19) Cave, R. J.; Newton, M. D. *Chem. Phys. Lett.* **1996**, *249*, 15–19.
- (20) Locknar, S. A.; Peteanu, L. A. *J. Phys. Chem. B* **1998**, *102*, 4240–4246.
- (21) Liptay, W. Dipole Moments and Polarizabilities of Molecules in Excited Electronic States. In *Excited States*; Lim, E. C., Ed.; Academic Press: New York, 1974; pp 129–229.
- (22) Premvardhan, L.; Peteanu, L. *Chem. Phys. Lett.* **1998**, *296*, 521–529.
- (23) Premvardhan, L. L.; Peteanu, L. A. *J. Phys. Chem. A* **1999**, *103*, 7506–7514.
- (24) Solomon, E. I.; Hare, J. W.; Dooley, D. M.; Dawson, J. H.; Stephens, P. J.; Gray, H. B. *J. Am. Chem. Soc.* **1980**, *102*, 168–178.
- (25) Penfield, K. W.; Gewirth, A. A.; Solomon, E. I. *J. Am. Chem. Soc.* **1985**, *107*, 4519–4529.
- (26) The main uncertainty in this determination arises from the uncertainty in uniquely determining the position and intensity of this underlying transition which has a small oscillator strength relative to the main $S(\pi) \rightarrow \text{Cu}(d_{x^2-y^2})$ LMCT band.²⁴
- (27) Edington, M. D.; Diffey, W. M.; Doria, W. J.; Riter, R. E.; Beck, W. F. *Chem. Phys. Lett.* **1997**, *275*, 119–126.
- (28) Nar, H.; Messerschmidt, A.; Huber, R.; Van de Camp, M.; Canters, G. W. *J. Mol. Biol.* **1991**, *218*, 427.